

Ibrahim D.A., Al-Assam H., Jassim S., Du H. (2017) Multi-level Trainable Segmentation for Measuring Gestational and Yolk Sacs from Ultrasound Images. In: Valdés Hernández M., González-Castro V. (eds) Medical Image Understanding and Analysis. MIUA 2017. Communications in Computer and Information Science, vol 723. Springer, Cham

The final publication is available at Springer via [https://doi.org/10.1007/978-3-319-60964-5\\_8](https://doi.org/10.1007/978-3-319-60964-5_8)

# Using Trainable Segmentation and Watershed Transform for Identifying Unilocular and Multilocular Cysts from Ultrasound Images of Ovarian Tumour

Dheyaa Ahmed Ibrahim, Hisham Al-Assam, Hongbo Du, Sabah Jassim  
Department of Applied Computing, University of Buckingham, Buckingham, UK.  
(Dheyaa.Ibrahim@buckingham.ac.uk),

## ABSTRACT

Ovarian masses are categorised into different types of malignant and benign. In order to optimize patient treatment, it is necessary to carry out pre-operational characterisation of the suspect ovarian mass to determine its category. Ultrasound imaging has been widely used in differentiating malignant from benign cases due to its safe and non-intrusive nature, and can be used for determining the number of cysts in the ovary. Presently, the gynaecologist is tasked with manually counting the number of cysts shown on the ultrasound image. This paper proposes, a new approach that automatically segments the ovarian masses and cysts from a static B-mode image. Initially, the method uses a trainable segmentation procedure and a trained neural network classifier to accurately identify the position of the masses and cysts. After that, the borders of the masses can be appraised using watershed transform. The effectiveness of the proposed method has been tested by comparing the number of cysts identified by the method against the manual examination by a gynaecologist. A total of 65 ultrasound images were used for the comparison, and the results showed that the proposed solution is a viable alternative to the manual counting method for accurately determining the number of cysts in a US ovarian image.

## 1- INTRODUCTION

The lack of specific symptoms in ovarian cancer has been the leading cause of death from gynaecological cancers [1]. However, one of the most important aspects of treating this ‘silent killer’ is to accurately characterise and determine benign from malignant tumours. This determination is necessary to prevent unnecessary procedures, such as surgery, for those patients with benign masses whilst also allowing the optimisation of treatment for those with malignant masses. Nevertheless, it is still an arduous task to detect ovarian cancer in the early and treatable stages.

In order to characterise benign or malignant masses and distinguish the tumour types, ultrasound imaging has become the most widely used method due to its useful imaging characteristics, which can be separated into two aspects. The first aspect is the morphological features that are detailed on a B-mode image. These include unilocular and multilocular cysts, fluid, tumours, internal wall structure, papillary projections and acoustic shadows. The second beneficial aspect is the combined use of Doppler images to gain blood flow information. The results of these different aspects enable clinicians to determine the seriousness of the imaged mass [2] [3]. However, to gain a more accurate classification of tumour type, International Ovarian Tumour Analysis (IOTA) researchers created a model system that utilised sonography. These models include the Simple Rules, Risk of Malignancy Index (RMI), Logistic Regression models (LR1 and LR2) and the most recent ADNEX risk model [4].

In order to automatically extract these tumour characteristics, it is necessary to first segment the B-mode ultrasound image. However, accurate segmentation is largely determined by the quality of the image as artefacts, such as speckle, attenuation, signal dropout and shadows can make the task extremely complicated. These quality impacts can lead to boundaries being missed due to the presence of these artefacts and acquisition orientation of low contrast between the regions of interest [5].

The recent development of several novel ultrasound image segmentation algorithms has led to an increased focus on segmentation techniques. These algorithms are divided into five categories, which are thresholding [6], clustering [7], edge detection [8], region growing [9] and trainable segmentation [10]. Whilst these algorithms have shown significant success in many applications, one has yet to be developed that can be applied to all images. Indeed, many of these algorithms have shown suitability for a particular application rather than a general applicability across all applications. The simplicity and

efficiency of the thresholding methods makes them an appealing choice. Nevertheless, these algorithms are unable to separate different parts that have the same grey area. As the algorithms are based on traditional histograms, they are unable to process images with a closely unimodal histogram particularly in the cases where there is a significant difference in size between the target region and the background. Much improved segmentation results can be gained by employing clustering methods that partition an image into different regions of homogeneity. However, this type of methods is prone to over-segmentation; this must be addressed in to ensure effective feature extraction. One type of the most widely used segmentation algorithms is the edge detection method, which identifies points where there is an abrupt change in the greyscale level. However, the effectiveness of the methods reduces in images when the number of edges and closed curves or boundaries increases. These algorithms show improved results when compared to the thresholding algorithms using various image sets; nevertheless, the sequential nature of the typical region growing process limits its overall efficiency. This is because the produced regions are dependent on the scanned order of pixels and the values of the first scanned pixels that define a new segment.

The aforementioned problems associated with existing segmentation algorithms have led to the increased focus on developing accurate and more efficient image segmentation approaches. Whilst significant improvements have been made, there are still many obstacles that need to be overcome. This has encouraged the development of machine learning based solutions that extract regions of interest using pixel level classification made by classification models, such as a support vector machine or a neural network, trained from training data with known labels. The machine learning work as an attractive choice providing the system has a robust set of segmented training sample images [11].

This paper focuses on the use of cyst extraction from ultrasound images in order to make an identification of the tumour type. As the quality of the image dictates the success of the image segmentation, it is necessary to combine the initial segmentation stage of the neural network's trainable segmentation and the watershed transform in order to accurately establish the location and border of the area of interest. The trainable segmentation approach is presented in which the author details a two-class machine learning-based image segmentation technique that is capable of extracting the cysts from the image. After the initial learning stage, a neural network, trained classifier is able to carry out the segmentation process. Following this, the overlaying that occurs with watershed transform can then be solved using the distance function. The minimal grey value for each object is labelled using the h-minima and the border estimation between the overlapped objects is achieved through the application of the watershed transform. The results show that the proposed solution is a viable alternative to the manual counting method for accurately determining the number of cysts.

The rest of this paper is organised in four further sections. Section 2 describes the diagnosis of ovarian tumours. Section 3 describes in detail the proposed method. Section 4 evaluates the effectiveness of the proposed method with experimental data. Finally, Section 5 concludes the paper and outlines several possible ways to further improve the method.

## **2- OVARIAN TUMOUR DIAGNOSIS BASED ON ADNEX MODEL**

The Assessment of Different NEoplasias in the adneXa (ADNEX) model has been developed by scientists of the IOTA group. This model can differentiate between early and late stage (II-IV) primary cancers, secondary metastatic cancers, borderline tumours and benign tumours, with a risk percentage for each stage. The ADNEX model is based on six ultrasound parameters and three clinical parameters that offer risk calculation. The six ultrasound-image parameters used in the ADNEX model are: lesion diameter in mm, solid tissue proportion, number of papillary projections, number of cysts (10 or more, yes or no), the presence or absence of acoustic shadows, and the presence or absence of ascites. The three clinical parameters used are type of medical centre (oncology vs other hospital), age of patient in years, and serum CA125 level in  $\mu\text{ml}^{-1}$  in the blood [3]. Validation of the model was achieved using parameters collected by experienced ultrasound clinicians with a special interest in gynaecological ultrasonography, who were equivalent in experience and knowledge to UK radiology consultants (Education and Practical Standards Committee, European Federation of Societies for Ultrasound in Medicine and Biology (EFSUMB)). The benefit of this model is that it allows for effective patient triage due to its ability to identify the tumour stages. As such, patients can be rapidly assessed and propelled along the most suitable management pathways for their tumour stage, whether that is surgery, conservative follow-up or treatment at a specialist cancer unit. However, it is also beneficial to be able to identify the tumour malignancy sub-type as less aggressive treatment options are available for early-stage ovarian cancers and borderline ovarian tumours. This less aggressive treatment often allows younger women to retain their fertility. Identification of metastatic ovarian cancers should, nevertheless, be treated in the same manner as the primary cancer [3] [4].

This research specifically considers the automatic extraction of one particular ultrasound-image parameter from the list, i.e. the number of cysts.

### 3- PROPOSED METHOD

#### 3-1 Process Framework of the Proposed Method

Figure 1 below illustrates the process framework for the proposed method for automatic identification of ovarian cysts from static B-mode ultrasound images. To accurately locate a cyst within a given image, the process consists of two main steps. First, the neural network's trainable segmentation is able to isolate the cyst by carrying out the initial segmentation second, the watershed transform to distinguish the border. The paper presents a trainable segmentation approach devised by a formulation of a two-class machine learning-based image segmentation technique that is able to distinguish the cyst sac from the ultrasound image. The segmentation approach can be carried out by a trained classifier (neural network) after learning has occurred. Following this, the distance transform can be used as this considers the object shape and interior. The minimum grey value for each object in labelled using the application of h-minima (Marker-controlled) and the border estimation between the overlapped objects is carried out by watershed transform.

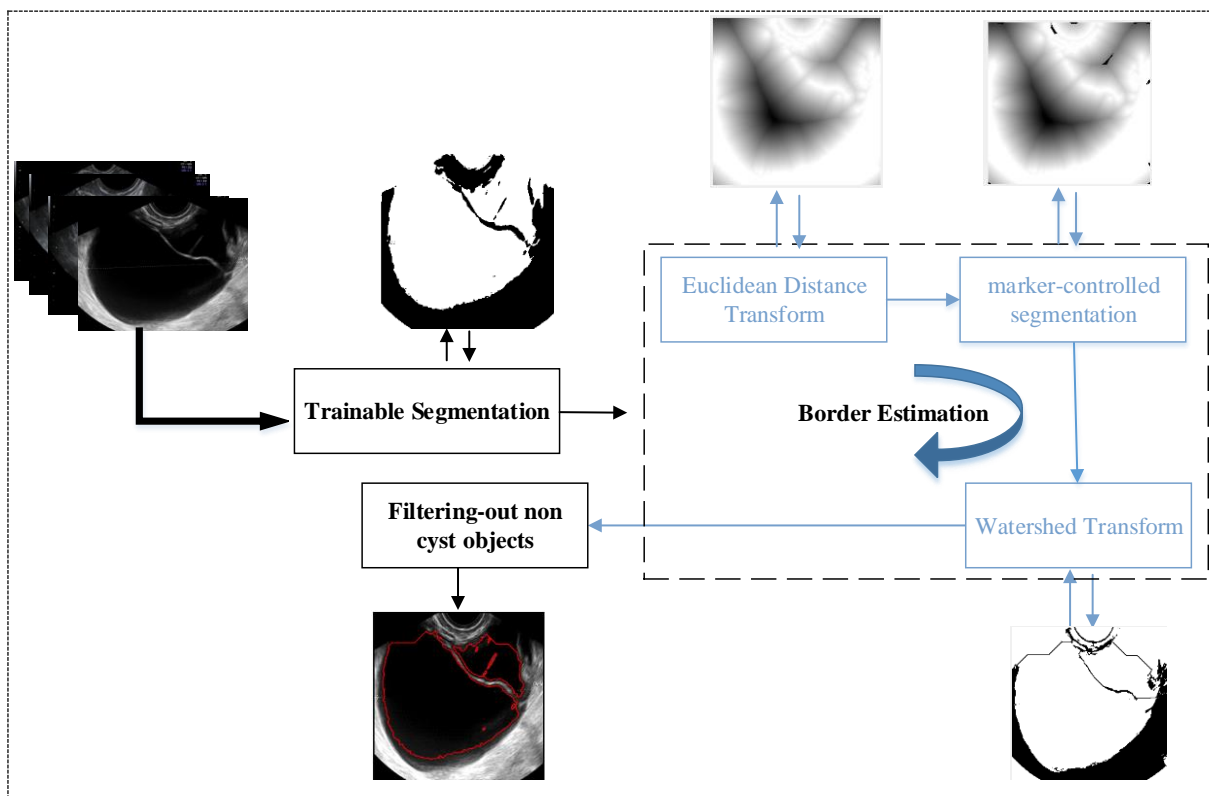


Figure 1: The proposed system

#### 3-2 Trainable Segmentation

The trainable segmentation aims to separate the region of interest (ROI), i.e. the tumour area, from the rest of the image. This process starts by collecting a number of training images each of which is then divided into a number of samples. A sample is a small square window of pixels of certain size, e.g. 3x3, taken either from areas inside (Class 1) or from areas outside (Class 2) the ROI. A set of HOG features (which are explained in detail later in this section) are then extracted from each window, forming a feature vector for the sample. A neural network classifier is then trained from this collection

of labelled feature vectors. After completion of the neural network training, an image to be segmented is scanned pixel by pixel. A small window of the same size, e.g. 3x3, is taken around each central pixel whereby the HOG feature vector is extracted from the window, and classified as being either inside or outside the ROI by the trained neural network. When the window is classified as being inside the ROI, the central pixel is then labelled also as being inside the ROI. Similarly, when the window is classified as being outside of the ROI, the central pixel is labelled as being outside. Once all the pixels of the image are labelled, the neighbouring pixels of “inside” class form the segmented ROI.

The HOG features, or histogram of oriented gradients, are general descriptors that are used for object identification in digital images. The feature extraction method was meant to quantify the occurrence of gradient orientation within a local image region. This is achieved by creating windows, or cells, around the pixels, and generating a local one-dimensional gradient direction or edge orientation histogram. This local histogram can then be contrast-normalised to improve invariance to shadowing and illumination [12] [13]. The whole process shows in Figure 2. Using this method, the shape and appearance of the object can be deduced by analysing the gradient intensity and edge directions within an image.

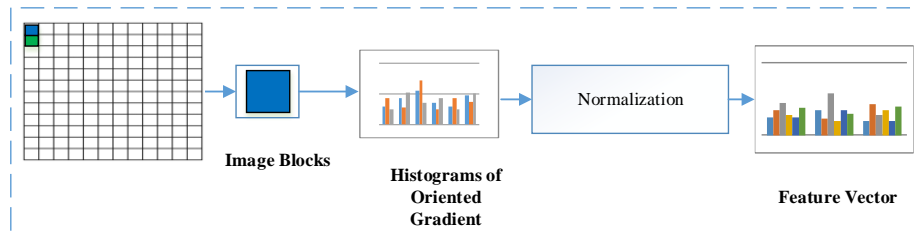


Figure 2: HOG process

### 3-3 Cyst Border Estimation

The estimation of the cysts border is achieved by using the binary image produced by the trainable segmentation stage as input. It is possible that separate objects may overlap. To differentiate the shapes of the individual objects all connected objects need to be separated. To estimate accurately the borders of the overlapping objects, this step of the proposed method involves a sequence of processing stages (see Figure 1), starting from Euclidean distance transform, followed by H-minima, and finally the watershed transform.

#### Euclidean distance transform and H-minimum (Marker-control)

Where overlapping objects is evident, a subsequent process of segmentation is needed after initial image segmentation which is able to detect these aggregates. Popular methods for aggregate detection and segmentation include the distance transform method [5] of aggregate associated binary images and watershed transform [6] application following the introduction of adequate markers. Binary image distance transform is determined in the following manner: every pixel  $x$  in set  $A$ ,  $DT(A)$  is its distance from  $x$  to the complement of  $A$ ,

$$DT(A)(X) = \min\{d(x, y), y \in A^c\} \quad (1)$$

A binary image’s distance transform is, therefore, calculated by assuming that  $A^c$  is the set of 1- valued pixels; this forms a greyscale image that can then be segmented using the watershed transform. However, unless the markers have been appropriately selected and applied, it has been shown that watersheds are prone to significant over-segmentation.

Figure 3 shows the effect of a typical distance transform calculation. The first ‘coarse’ segmentation generates a binary image of two overlapping objects (Figure.3(a)). However, the coarse segmentation does not separate overlapping objects, as such, it is possible to generate this binary image by using the neural network’s trainable. This binary image is then negated (Figure.3 (b)), before having the distance transform applied to generate the greyscale image in Figure 3(c). It can be seen here that the black region in Figure 3(b) that are the furthest from the white background appear as maxima. Despite this, several local maxima also appear as a result of figure morphology characteristics. By complementing the greyscale image in Figure 3(c), Figure 3(d) is generated giving a white background and the former maxima appear as minima. This method is described as an inner distance transform. The watershed transform is then applied to Figure 3(d) to generate

separation between the overlapped objects. It is possible to complement the region to be segmented outside of the aggregate to obtain adequate external markers. Over-segmentation causes the generation of the specious minima therefore it is necessary to ensure the construction of adequate markers.

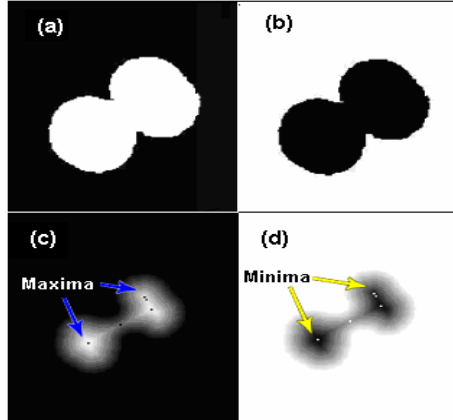


**Figure 3:** (a) Binary image from overlapping objects, (b) complemented binary image, (c) distance transform of the image in (b), and (d) complemented distance transform. Notice the maxima and minima indicated by arrows in (c) and (d).

It is possible to use several greyscale morphological functions when setting the inner marker process; this will control the negative effects of specious minima prior to the application of the watershed transform. These morphological functions include:

- The imposition of minima at specific points by inserting a  $-\infty$  value in a specific position to eliminate the existence of local minima in other points within the greyscale image. When these are placed in appropriate points, effective markers are created.
- From the result of the inner distance transform, the  $H$ -minima can be applied to eliminate all of the minima with a depth that is equal to or less than a given positive threshold. This will reduce the remaining minima's depth within the magnitude of the threshold, therefore local minima can be eliminated by using an appropriate threshold and the generated regional minima can be used as effective markers.

The implementation of this method can be completed using a morphological sup-geodesic reconstruction  $\nabla D$  of the surface intensity of the image  $f$ .  $h$  determines the surface increased by the threshold and the structuring element that defines the connectivity is  $D$  [14] [15].

$$HMIN_{h,D}(f) = f(\nabla_D(f + h)) \quad (2)$$

Despite this simplistic description, the actual task of determining appropriate H-minima transform thresholds and identification of a suitable place to impose a minimum is complex and non-trivial. It is easy to misplace the markers thereby allowing specious minima to remain. Additionally, regional minima can merge thereby preventing marker isolation. By analysing it can be seen that the actual task requires the elimination of specious minima as well as the minimum in the blob connections. This needs to be done whilst simultaneously maintaining the isolation of the two minima that reside at the approximate centre of the overlapping objects that need to be segmented.

### Watershed Transform

In order to achieve initial separation between the overlapped objects, this paper utilises the application of the fast immersion-based watershed transform formulated by Vincent and Soile [16] on the output of the gradient-weighted distance transform. As illustrated in Figure 1, the watershed transform helps in closing the border of the cyst (see the output of the watershed compared with the output of the trainable segmentation in Figure 1).

## 4- RESULTS & EVALUATION

### 4-1 Dataset

All static ultrasound images of ovarian tumours used in this study are the results of ultrasound scans conducted on women recruited into the IOTA study. All women in this study underwent surgical removal of the tumours between November 2005 and November 2013 with a known histological diagnosis. They all signed a written informed consent form to allow the use and analyse the data for research purposes. For this study, a 2D B-mode ultrasound image of a surgically removed adnexal mass was used, due to its representation of the final histopathology. We retrieved a total of 65 ultrasound images of 65 anonymous patients from the IOTA database (Astraia software gmbh, Germany) at the Department of Gynaecological Ultrasonography, Campus Gasthuisberg, KU Leuven, Belgium. Each image is a 2D B-mode ultrasound scan image of the surgically removed tumours.

### 4-2 Result

To obtain a ground truth to evaluate the effectiveness of our proposal, a domain expert was asked to manually count the number of cysts in 65 ultrasound images. This is then used as a ground truth to compare the automatic measurements against. We found that 54 out of 65 images were accurately segmented and produced the correct number of cysts with and 11 images producing incorrect number of cysts. Therefore, the success rate of producing the correct number of cysts is around 83%. Figure 4 shows a more detailed comparison between manual and automatic measurements in relation to the number of cysts in each ultrasound image. The blue part of the automatic counting represents the true positive (i.e. the number of images that have a correct cyst count) whereas the red part represents the false positive (i.e. the number of images that have inaccurate cyst count).

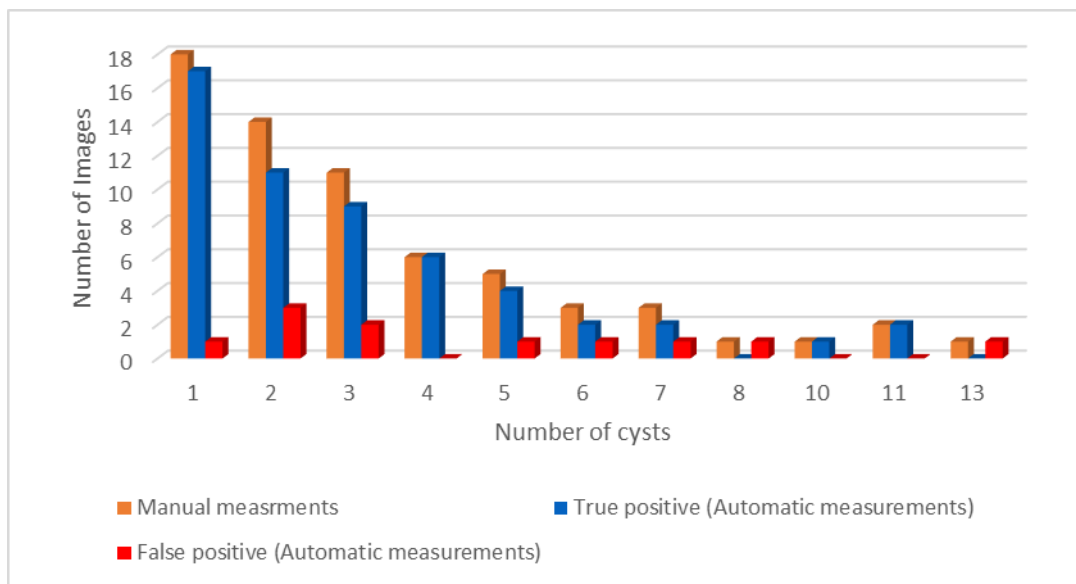


**Figure 4:** Cyst counting- Automatic vs. Manual

### 4-3 Evaluation of the Proposed Method

As we mention previously, this paper aims to companies the trainable segmentation with watershed transform to binarize the image and reconstruct the missing border. To analyse the performance of the proposed segmentation algorithm, the trainable segmentation utilised a 2-layer back-propagation neural network that was trained with 100 sample regions generated from 8 training images.

Border estimation by mathematical morphology is a methodology based upon the notions of watershed transform. Unfortunately, this transform leads to an over segmentation problem. To overcome this problem, a marker-control strategy has been used. This technique is based on the idea which machine vision system knows from other source the entail location of the objects to be located. Figure 5 shows that the link between the border estimation techniques is very important. i.e. if we applied the watershed transform directly on the binary image we will have an over-segmentation problem. Therefore, using the Euclidian distance transform is a way to define the properties which will be used to mark the objects.

Figure 5 shows the experimental results whilst Figure 5.a displays a benign mass' ROI and Figure 5.b shows that result of the trainable segmentation. The results generated using border estimation are shown respectively in Figures 5.c-f. As such, the proposed algorithm displayed superior results with accurate boundary outlines and an overall better performance.

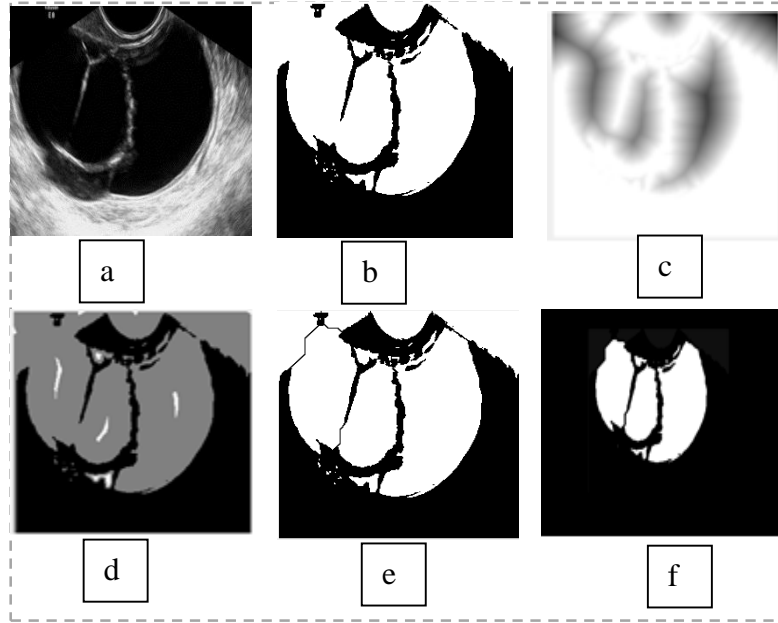


**Figure 5:** Segmentation Result, (a) original image, (b) trainable segmentation, (c) distance transform, (d) H-minima, watershed transform, (e) segmented image

## 5- CONCLUSION

This paper presented a novel approach for automatic segmentation of ovarian cysts from static B-mode ultrasound images to count the number cysts in the image, which is a strong indicator of the type of the underlying tumour. The paper highlighted the difficulties associated with segmentation of such images that arise from the colour intensities overlap between of the cyst and those of the background tissues. The segmentation framework starts with a trainable segmentation to identify the tumor areas followed by distance and watershed transforms to estimate the cyst borders. The results showed that the proposed solution was able to generate a good estimation of the number of cysts. Indeed, the results showed a closely comparable results with obtained manual by a domain experts.

## Reference

- [1] K. Chan and T. Selman, "Testing for ovarian cancer," Best practice & research Clinical obstetrics & gynaecology, vol. 20, no. 6, pp. 977-983, 2006.

- [2] A. Sayasneh, C. Ekechi, L. Ferrara, J. Kaijser, C. Stalder, S. Sur, D. Timmerman and T. Bourne, "The characteristic ultrasound features of specific types of ovarian pathology (Review)," *International journal of oncology*, vol. 46, no. 2, pp. 445-458, 2015.
- [3] A. Sayasneh, L. Ferrara, B. De Cock, S. Saso, M. Al-Memar, S. Johnson, J. Kaijser, J. Carvalho, R. Husicka, A. Smith and others, "Evaluating the risk of ovarian cancer before surgery using the ADNEX model: a multicentre external validation study," *British Journal of Cancer*, vol. 115, no. 5, pp. 542-548, 2016.
- [4] B. Van Calster, K. Van Hoorde, L. Valentin, A. C. Testa, D. Fischerova, C. Van Holsbeke, L. Savelli, D. Franchi, E. Epstein, J. Kaijser and others, "Evaluating the risk of ovarian cancer before surgery using the ADNEX model to differentiate between benign, borderline, early and advanced stage invasive, and secondary metastatic tumours: prospective multicentre diagnostic study," *Bmj*, vol. 349, p. g5920, 2014.
- [5] J. A. Noble and D. Boukerroui, "Ultrasound image segmentation: a survey," *IEEE Transactions on medical imaging*, vol. 25, no. 8, pp. 987-1010, 2006.
- [6] D. A. Ibrahim, H. Al-Assam, H. Du, J. Farren, D. Al-karawi, T. Bourne and S. Jassim, "Automatic segmentation and measurements of gestational sac using static B-mode ultrasound images," in *SPIE Commercial+ Scientific Sensing and Imaging*, 2016.
- [7] D. Boukerroui, O. Basset, N. Guerin and A. Baskurt, "Multiresolution texture based adaptive clustering algorithm for breast lesion segmentation," *European Journal of Ultrasound*, vol. 8, no. 2, pp. 135-144, 1998.
- [8] Y. Yu and S. T. Acton, "Edge detection in ultrasound imagery using the instantaneous coefficient of variation," *IEEE Transactions on Image processing*, vol. 13, no. 12, pp. 1640-1655, 2004.
- [9] S. Poonguzhali and G. Ravindran, "A complete automatic region growing method for segmentation of masses on ultrasound images," in *Biomedical and Pharmaceutical Engineering, 2006. ICBPE 2006. International Conference on*, 2006.
- [10] C. Kotropoulos and I. Pitas, "Segmentation of ultrasonic images using support vector machines," *Pattern Recognition Letters*, vol. 24, no. 4, pp. 715-727, 2003.
- [11] K. Sakthivel, R. Nallusamy and C. Kavitha, "Color Image Segmentation Using SVM Pixel Classification Image," *World Academy of Science, Engineering and Technology, International Journal of Computer, Electrical, Automation, Control and Information Engineering*, vol. 8, no. 10, pp. 1919-1925, 2015.
- [12] N. Dalal and B. Triggs, "Histograms of oriented gradients for human detection," in *2005 IEEE Computer Society Conference on Computer Vision and Pattern Recognition (CVPR'05)*, 2005.
- [13] M. S. S. Patil, M. A. Junnarkar and M. D. Gore, "Study of Texture Representation Techniques," *image*, vol. 3, no. 3, 2014.
- [14] P. Soille, *Morphological image analysis: principles and applications*, Springer Science & Business Media, 2013.
- [15] L. L. G. J. V. China Valdés, "EVALUATION OF DISTANCE TRANSFORM BASED ALTERNATIVES FOR IMAGE SEGMENTATION OF OVERLAPPING OBJECTS".
- [16] L. Vincent and P. Soille, "Watersheds in digital spaces: an efficient algorithm based on immersion simulations," *IEEE transactions on pattern analysis and machine intelligence*, vol. 13, no. 6, pp. 583-598, 1991.